Bulletin of the Seismological Society of America, Vol. 102, No. 2, pp. 873–877, April 2012, doi: 10.1785/0120110181

Short Note

Temporal Stability of Coda Q^{-1} in Southern California

by Laura E. Sumiejski and Peter M. Shearer

Abstract Some studies of coda Q^{-1} have found temporal changes that may be associated with earthquake activity, but these analyses are subject to biases due to differences in source locations and other nonstationary behavior in earthquake catalogs. These biases can be greatly reduced by using clusters of repeating earthquakes; studies using this approach have generally found no resolvable changes in coda Q^{-1}. We examine coda Q^{-1} variations across southern California using 22 similar event clusters identified from a recent large-scale waveform cross-correlation project to improve earthquake locations. These clusters are found across the region and span the time period between 1981 and 2005. We apply the method of Beroza *et al.* (1995) to compute differential coda Q^{-1} using waveforms from similar earthquake pairs and analyze the results to constrain any possible temporal variations. Results from individual event pairs show a great deal of scatter in differential coda Q^{-1}, but exhibit no clear temporal variations or changes associated with large earthquakes. Application of a median filter to smooth the results shows that any persistent large-scale changes in coda Q^{-1} during this time period are less than about 30%.

Introduction

Seismic coda waves are scattered waves resulting from heterogeneities in the earth (e.g., Aki, 1969; Aki and Chouet, 1975). *S*-wave coda from local earthquakes is caused by heterogeneity in the lithosphere and typically exhibits an exponential decay in amplitude that can be characterized in terms of coda Q^{-1} (Q_c^{-1}), defined as

$$A(t) = \frac{k}{t}\exp\left[\frac{-\omega t}{2}Q_c^{-1}\right], \tag{1}$$

where A is the amplitude of the seismogram, k is a scaling factor, t is the time since the origin of the earthquake, ω is the angular frequency, and Q_c^{-1} is the coda Q^{-1}.

Because scattering properties might change as cracks open or close in response to stress changes occurring before or after earthquakes, a number of studies have examined whether temporal changes in Q_c^{-1} can be resolved. Some studies found evidence for changes in coda Q^{-1} prior to earthquakes (e.g., a decrease in coda Q^{-1} of 50%–70% by Jin and Aki, 1986 and a decrease of 25%–29% by Su and Aki, 1990). Others noted a change between the coda Q^{-1} just before and immediately after the earthquake, rather than a precursory change. Peng *et al.* (1987) found this change to be a 20%–30% increase close to the mainshock and a decrease farther from the mainshock. Tsukuda (1988) found the changes to be around 20%, Wang *et al.* (1989) recorded a 40% increase in Q_c^{-1}, and Huang and Kisslinger (1992) found a 10% decrease in coda Q^{-1}. However, other studies have found no temporal variations in coda Q^{-1}, either around large earthquakes or in general across a region over some span of time (Huang and Wyss, 1988; Woodgold, 1994; Hellweg *et al.*, 1995; Tselentis, 1997). The apparent temporal variations that have been found in some Q_c^{-1} studies might instead be artifacts due to differences in hypocenter locations and other source characteristics (Beroza *et al.*, 1995; Aster *et al.*, 1996; Antolik *et al.*, 1996; Chen and Long, 2000).

To eliminate these possible biasing effects, it is desirable to examine repeatable sources in nearly the same location. Beroza *et al.* (1995) looked at earthquake doublets in order to solve for the change in coda Q^{-1} rather than directly for Q_c^{-1} itself, and in doing so, eliminated many factors that may cause an apparent temporal change in Q_c^{-1}. The difference in coda Q^{-1} from two earthquakes can be found by taking the ratio of the amplitudes,

$$\frac{A_i}{A_j} = \frac{k_i}{k_j}\exp\left[\frac{-\omega t}{2}(Q_i^{-1} - Q_j^{-1})\right], \tag{2}$$

where i and j refer to different events. Taking the natural logarithm of equation (2) gives the equation for a straight line for amplitude ratio versus time:

$$\begin{aligned}\ln\left(\frac{A_i}{A_j}\right) &= \ln\left(\frac{k_i}{k_j}\right) + \frac{\omega t}{2}(Q_j^{-1} - Q_i^{-1}) \\ &= \ln\left(\frac{k_i}{k_j}\right) + \frac{\omega t}{2}\Delta Q_c^{-1},\end{aligned} \tag{3}$$

where the slope is proportional to the change in coda Q^{-1} (ΔQ_c^{-1}) (Beroza *et al.*, 1995).

Using earthquake doublets, Beroza *et al.* (1995) found no resolvable temporal change in coda Q^{-1} in the vicinity of the 1989 Loma Prieta earthquake (M_w 6.9) in California. Their results limited any Q_c^{-1} change to no more than 5%, much less than studies that had reported precursory variations in Q_c^{-1} for other earthquakes. A similar study in the Parkfield, California, region used clusters of repeating earthquakes and also found temporal changes no greater than 5% (Aster *et al.*, 1996; Antolik *et al.*, 1996).

However, these studies have covered only limited regions, and it is possible that coda Q^{-1} might vary in other areas. To systematically examine coda Q^{-1} stability across southern California, we adopt the Beroza *et al.* (1995) method to analyze 22 similar event clusters in southern California (see Fig. 1), which are a spatially diverse subset of the clusters identified by Lin *et al.* (2008) in a recent large-scale waveform cross-correlation project. Seismograms from the events in each cluster are similar but not wiggle-for-wiggle identical, especially in the coda. The clusters contain events that span a period of 25 years, between 1981 and 2005, during which time there were several large earthquakes. Our results show no resolvable temporal changes in coda Q^{-1} during this time period, at the level of ±30%.

Method

From the similar event clusters identified by Lin *et al.* (2008) using waveform cross-correlation, we initially selected 95 clusters that contained events that spanned the full 1981–1995 time period. For each cluster we obtained Southern California Seismic Network waveforms from the Southern California Earthquake Data Center (SCEDC), and then cross-correlated station P waveform pairs for every event pair (Fig. 2a). Prior to cross correlation, the data were filtered to between 1 and 10 Hz, which Hauksson and Shearer (2005) and Lin *et al.* (2007) found gives good results

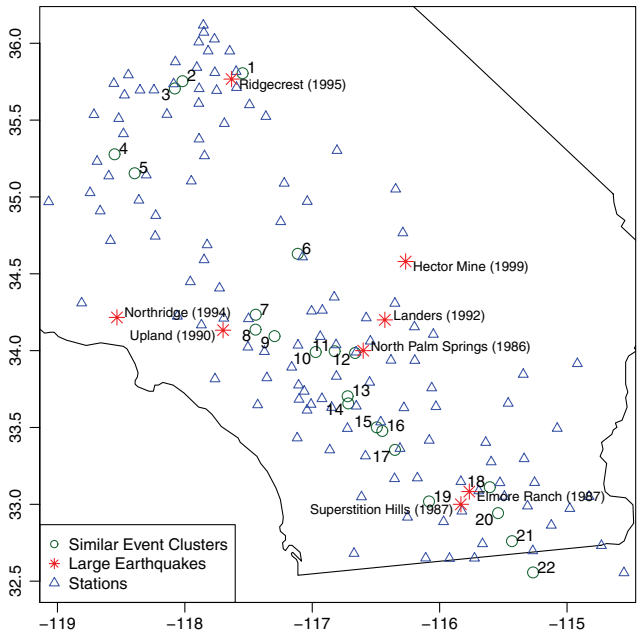

Figure 1. A map of southern California showing the 22 similar event clusters (circles) analyzed in this study and the stations (triangles) that recorded them. The stars show major earthquakes. The color version of this figure is available only in the electronic edition.

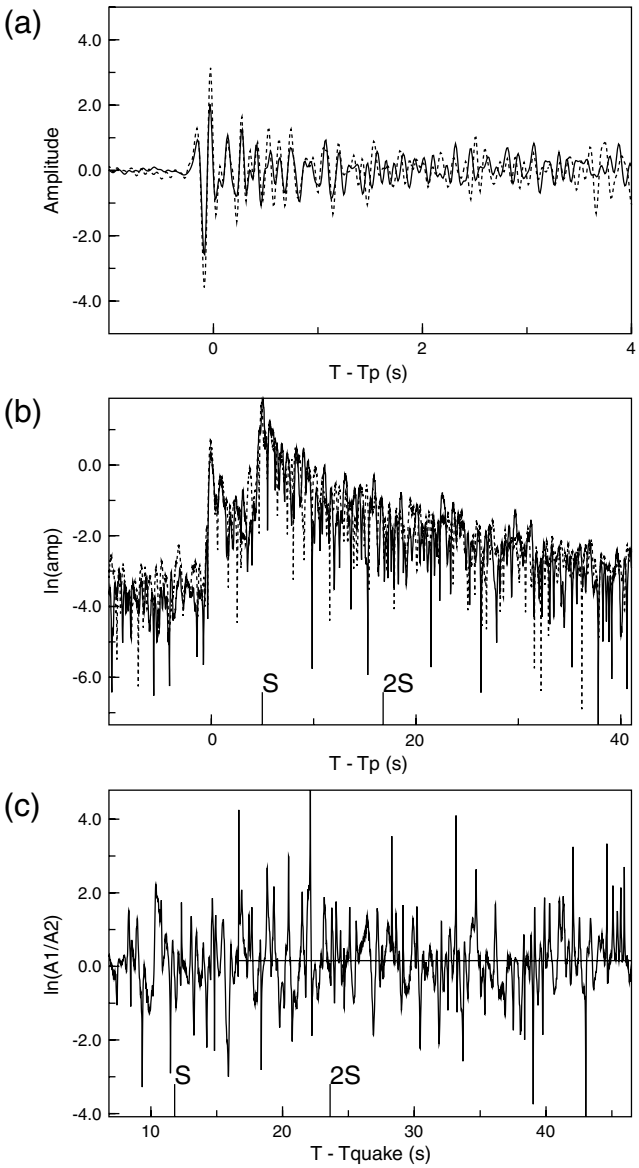

Figure 2. An example showing how a pair of similar earthquakes is processed. (a) The cross-correlated and aligned P waves, with event 1 shown as a dashed line and event 2 as a solid line. Time is relative to the predicted P arrival time. (b) The corresponding envelope functions for the two earthquakes, aligned using the cross-correlation results. Natural log amplitude is plotted. The S time and twice the S time are marked. (c) The natural log of the ratio of the envelope amplitudes and the best-fitting line (starting at 1.4 times the S time). The slope of the fitted line is proportional to ΔQ_c^{-1}.

for *P*-wave timing. We use vertical component data, except for cluster 10 (see Fig. 1), for which we use horizontal component data for two stations. For each cluster, we examine the correlation coefficients to determine which event has the highest correlation with all the other events within the cluster. This event is used as a control event to which we compare all the other events in the cluster. For each waveform pair we then determine the change in coda Q^{-1} using the Beroza *et al.* (1995) approach described previously. This provides ΔQ_c^{-1} estimates for each event (excluding the control event) with respect to the control event.

We only use waveform pairs with a correlation coefficient greater than 0.6, which limits the number of measurements we obtain per cluster. Almost all the event magnitudes are between 0.5 and 3. We band-pass filter the data between 4 and 8 Hz for our selected pairs and compute an envelope function for each waveform. We selected this passband because it has generally good signal-to-noise in our waveforms, which permits resolving *S* coda to longer times than at other frequencies. The envelope function is computed from

$$A_e(t) = \sqrt{A(t)^2 + H(t)^2}, \tag{4}$$

where A is the amplitude of the seismogram at time t, and H is the Hilbert transform of the amplitude (e.g., Kanasewich, 1973). We then align the seismograms and their envelope functions using the time shift from the cross-correlation results (Fig. 2b).

We analyze the *S* coda amplitude in a time window between 1.4 times the *S*-wave travel time to when the coda signal from one of the two waveforms drops below 1.4 times the noise level (this signal-to-noise measure is defined as the ratio of the average signal in a 5-s running window to the average pre-*P*-wave noise). The window length is computed separately for each waveform pair and thus is not of fixed length for any event. We then fit a line to the amplitude ratio between the two envelope functions from equation (3) to estimate the possible changes in Q_c^{-1} (Fig. 2c). Because the amplitude ratio can have extreme values, for robustness we use an L1-norm fitting method. To provide a reasonably well-constrained slope estimate, we use measurements only when the time window for the fit is at least 8 s.

The resulting estimates contain a large amount of scatter, which likely is not due to changes in coda Q^{-1}, but reflects the fact that although the waveforms for the event pairs have similar shaped *P* waves, they are not identical, particularly in the coda. To reduce this scatter, we assume any real changes in coda Q^{-1} will occur over relatively long time periods so that we can temporally smooth the results for individual events. To do this, we first remove the median for the entire cluster to remove any potential bias from the choice of the reference event and then calculate the median values over yearly intervals. To estimate errors for the median values, we use a bootstrap method to randomly resample (with replacement) the ΔQ_c^{-1} values within each year and compute the median from each resampled dataset. Using 1000 bootstrap

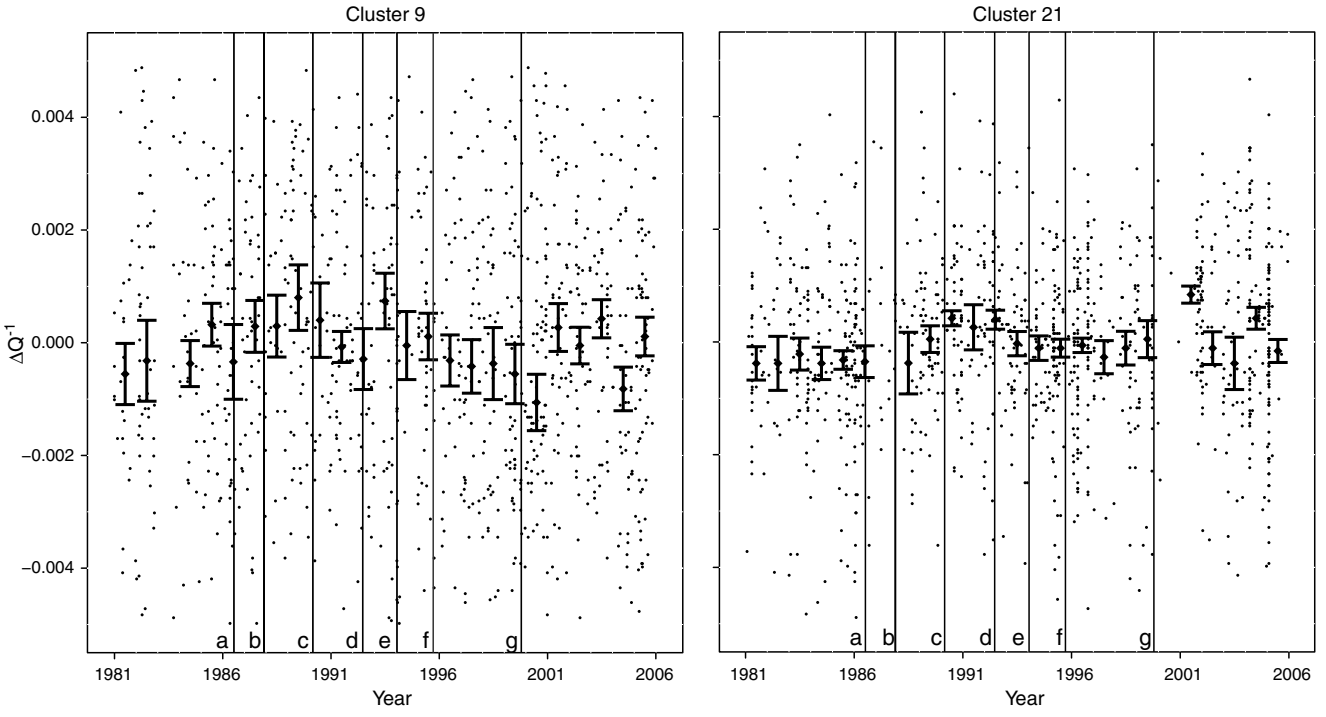

Figure 3. ΔQ_c^{-1} (small black dots) for similar events in (left) cluster 9 and (right) cluster 21. The black diamonds are the medians calculated for yearly intervals of ΔQ_c^{-1}. The error bars show estimated standard errors for the median values. The vertical lines indicate major earthquake occurrence times for a, North Palm Springs; b, Elmore Ranch; c, Upland; d, Landers; e, Northridge; f, Ridgecrest; and g, Hector Mine. A few of the ΔQ_c^{-1} values exceed the bounds of ±0.005 that are shown here.

resamples, we estimate the standard error from the standard deviation of the resulting medians. Figure 3 shows two clusters with the calculated medians and estimated errors. To obtain stable results, we only show results where we have at least 20 data points per year. This requirement, together with the correlation coefficient and fitting window cutoffs discussed previously, reduces the number of similar event clusters from our original 95 to 22 that provide adequate temporal coverage. Each of these remaining clusters spans most, if not all, of the 25 years for which we have data, as well as having a good geographical spread in southern California and greater than 20 data points in each year for most years (Fig. 4). For convenience, we have reassigned the cluster numbers in Lin *et al.*'s (2007) LSH catalog to the 22 numbers used here. The corresponding original LSH cluster numbers are (1 to 22): 562, 474, 923, 560, 751, 376, 206, 616, 1514, 22, 456, 846, 309, 25, 1, 153, 144, 868, 771, 197, 179, 1466.

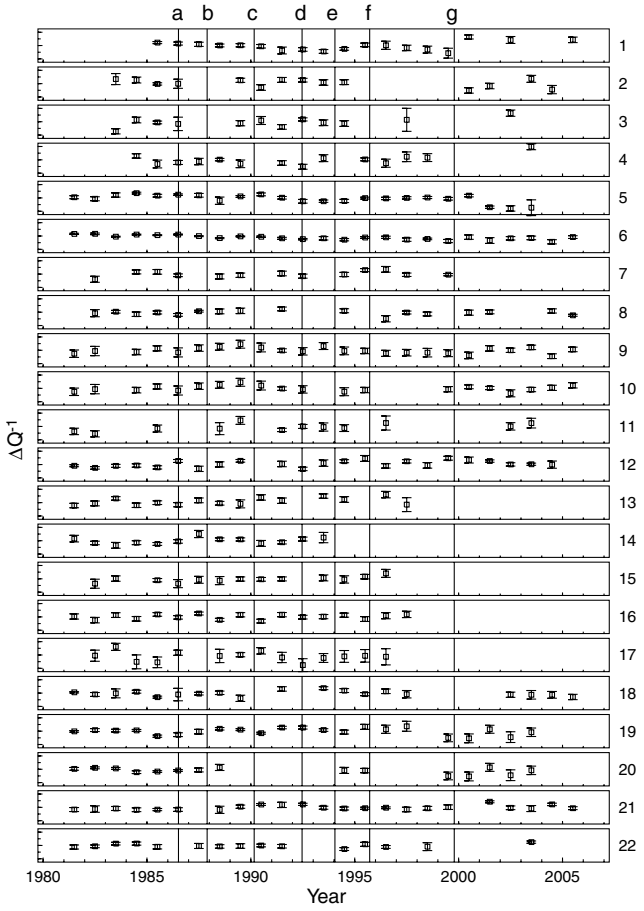

Figure 4. The median values (black diamonds) and their estimated standard errors for ΔQ_c^{-1} calculated over yearly intervals for the 22 similar event clusters analyzed in this study. The *y*-scale for each plot ranges from −0.0025 to 0.0025. The cluster numbers are show on the right. The vertical lines show major earthquake occurrence times for a, North Palm Springs; b, Elmore Ranch; c, Upland; d, Landers; e, Northridge; f, Ridgecrest; and g, Hector Mine.

Results

Figure 4 shows results for the 22 similar event clusters we analyzed in detail. The yearly median value of ΔQ_c^{-1} found for all of the clusters varies between ± 0.002, with over 90% of the values between ± 0.001 (Fig. 5). There is no systematic temporal trend in ΔQ_c^{-1} for any of the clusters or a clear change associated with any of the large earthquakes. Because the yearly bins include some events from both before and after the large earthquakes, there is a possibility that coseismic changes in Q_c^{-1} could be blurred by this time averaging. To check for this, we also computed a version of Figure 4, in which the bin boundaries are adjusted to exactly coincide with the large earthquake times. This plot appears very similar to the original and shows no evidence for changes in Q_c^{-1} caused by the earthquakes.

Coda Q is generally observed to increase with frequency (e.g., Phillips and Aki, 1986). Using the Phillips and Aki (1986) value of $Q_c \sim 300$ at 6 Hz for short time windows in central California, the ΔQ_c^{-1} variations of ± 0.001 translate to $\pm 30\%$ variations in absolute coda Q^{-1}. We thus see no evidence to support any changes in coda Q^{-1} in southern California during the 1981 to 2005 time period as large as those identified by Jin and Aki (1986) and Su and Aki (1990), or any changes associated with the occurrence of large earthquakes. However, our constraints on coda Q^{-1} are not as tight as the negative results reported by Beroza *et al.* (1995), Aster *et al.* (1996), and Antolik *et al.* (1996). This is likely due to the fact that the event clusters that we analyzed do not contain earthquakes as similar as those used in the other studies. It is possible that better results could be obtained by increasing the minimum correlation coefficient that we require, at the cost of decreasing the number of events. It does not appear that southern California contains as many nests of nearly identical earthquakes as are found on the San Andreas fault in central California.

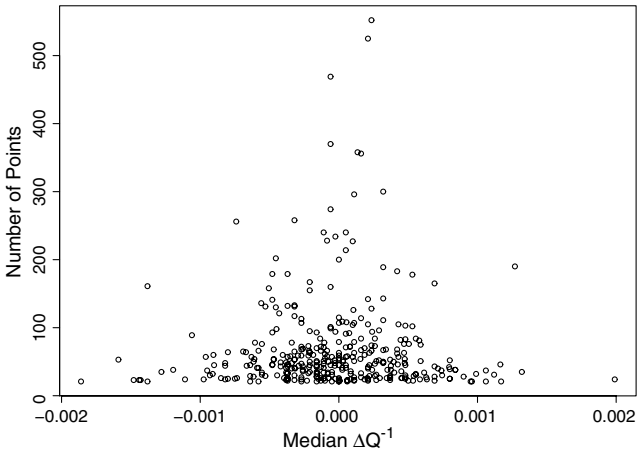

Figure 5. The median values calculated over yearly intervals versus the number of points used to calculate each median value. The more points used in the calculation, the more accurate the resulting median value.

Our results finding no clear temporal variations in coda Q^{-1} in southern California are consistent with the recent study of Lin *et al.* (2008), which analyzed travel times from similar event clusters to show that any large-scale, long-lasting temporal variations in P and S velocities across southern California are less than $\pm 0.2\%$. Our constraints on possible scattering properties related to coda Q^{-1} variations are less precise but are similar in geographical and temporal coverage. Both studies suggest that the observable large-scale seismic properties of the southern California crust have been stable since the early 1980s, although we cannot rule out the possibility of variations smaller than the spatial or temporal resolving power of the methods.

Data and Resources

We thank Peggy Hellweg and an anonymous reviewer for their constructive comments. Seismograms used in the study were downloaded using the SCEDC Seismic Transfer Program. Some figures were made using R: A language and environment for statistical computing, including the R packages maps (http://www.r-project.org/; last accessed December 2011) and ggplot2 (© Hadley Wickham 2011 from http://had.co.nz/ggplot2/; last accessed December 2011). This research was supported by the USGS/NEHRP program and by the Southern California Earthquake Center.

References

Aki, K. (1969). Analysis of the seismic coda of local earthquakes as scattered waves, *J. Geophys. Res.* **74,** 615–631.

Aki, K., and B. Chouet (1975). Origin of coda waves: Source, attenuation, and scattering effects, *J. Geophys. Res.* **80,** 3322–3342.

Antolik, M., R. M. Nadeau, R. C. Aster, and T. V. McEvilly (1996). Differential analysis of coda Q using similar microearthquakes in seismic gaps. Part 2: Application to seismograms recorded by the Parkfield high resolution seismic network, *Bull. Seismol. Soc. Am.* **86,** 890–910.

Aster, R. C., G. Slad, J. Henton, and M. Antolik (1996). Differential analysis of coda Q using similar microearthquakes in seismic gaps. Part 1: Techniques and application to seismograms recorded in the Anza seismic gap, *Bull. Seismol. Soc. Am.* **86,** 868–889.

Beroza, G. C., A. T. Cole, and W. L. Ellsworth (1995). Stability of coda wave attenuation during the Loma Prieta, California, earthquake sequence, *J. Geophys. Res.* **100,** 3977–3987.

Chen, X., and L. T. Long (2000). Hypocenter migration as an explanation for temporal changes in coda Q, *J. Geophys. Res.* **105,** 16,151–16,160.

Hauksson, E., and P. Shearer (2005). Southern California hypocenter relocation with waveform cross-correlation, Part 1: Results using the double-difference method, *Bull. Seismol. Soc. Am.* **95,** 896–903.

Hellweg, M., P. Spudich, J. B. Fletcher, and L. M. Baker (1995). Stability of coda Q in the region of Parkfield, California: View from the U.S. Geological Survey Parkfield dense seismograph array, *J. Geophys. Res.* **100,** 2089–2102.

Huang, Z.-X., and C. Kisslinger (1992). Coda-Q before and after the 1986 Andreanof Islands earthquake, *Pure Appl. Geophys.* **138,** 1–16.

Huang, Z.-X., and M. Wyss (1988). Coda Q before the 1983 Hawaii ($M_S = 6.6$) earthquake, *Bull. Seismol. Soc. Am.* **78,** 1279–1296.

Jin, A., and K. Aki (1986). Temporal change in coda Q before the Tangshan earthquake of 1976 and the Haicheng earthquake of 1975, *J. Geophys. Res.* **91,** 665–673.

Kanasewich, E. R. (1973). *Time Series Analysis in Geophysics*, University of Alberta Press, Edmonton, Alberta, Canada.

Lin, G., P. M. Shearer, and E. Hauksson (2007). Applying a three-dimensional velocity model, waveform cross correlation, and cluster analysis to locate southern California seismicity from 1981 to 2005, *J. Geophys. Res.* **112,** doi 10.1029/2007JB004986.

Lin, G., P. M. Shearer, and E. Hauksson (2008). A search for temporal variations in station terms in Southern California from 1984 to 2002, *Bull. Seismol. Soc. Am.* **98,** 2118–2132.

Peng, J.-Y., K. Aki, B. Chouet, P. Johnson, W. H. K. Lee, S. Marks, J. T. Newberry, A. S. Ryall, S. W. Stewart, and D. M. Tottingham (1987). Temporal change in coda Q associated with the Round Valley, California, earthquake of November 23, 1984, *J. Geophys. Res.* **92,** 3507–3526.

Phillips, W. S., and K. Aki (1986). Site amplification of coda waves from local earthquakes in central California, *Bull. Seismol. Soc. Am.* **76,** 627–648.

Su, F., and K. Aki (1990). Temporal and spatial variation on coda Q^{-1} associated with the North Palm Springs earthquake of July 8, 1986, *Pure Appl. Geophys.* **133,** 23–52.

Tselentis, G. A. (1997). Evidence for stability in coda Q associated with the Egion (central Greece) earthquake of 15 June 1995, *Bull. Seismol. Soc. Am.* **87,** 1679–1884.

Tsukuda, T. (1988). Coda-Q before and after the 1983 Misasa earthquake of M 6.2, Tottori Prefecture, Japan: Scattering and attenuation of seismic waves, *Pure Appl. Geophys.* **128,** 261–279.

Wang, J. H., T. L. Teng, and K. F. Ma (1989). Temporal variation of coda Q during Hualien earthquake of 1986 in eastern Taiwan, *Pure Appl. Geophys.* **130,** 617–634.

Woodgold, C. R. D. (1994). Coda Q in the Charlevoix, Quebec, region: Lapse-time dependence and spatial and temporal comparisons, *Bull. Seismol. Soc. Am.* **84,** 1123–1131.

Institute of Geophysics and Planetary Physics
Scripps Institution of Oceanography
University of California–San Diego
La Jolla, California 92093-0225

Manuscript received 22 June 2011